# A Steady-State Mass Balance Model of the Polycarbonate–$CO_2$ System Reveals a Self-Regulating Cell Growth Mechanism in the Solid-State Microcellular Process

M. R. HOLL, J. L. GARBINI, W. R. MURRAY, V. KUMAR

Department of Mechanical Engineering, University of Washington, Seattle, Washington 98195

*Received 20 September 1999; revised 16 January 2001; accepted 26 January 2001*
*Published online 28 February 2001*

**ABSTRACT:** A simple mechanism regulating polymer mobility is demonstrated to determine initial and final growth states of solid-state microcellular foams. This mechanism, governed by the extent of plasticization of the polymer by the dissolved gases, is examined with a mass balance model and results from foam growth experiments. Polycarbonate was exposed to $CO_2$, which acted as both a plasticizing gas and a physical blowing agent driving foam growth. The polycarbonate specimens were saturated to the equilibrium gas concentration at 25 °C for $CO_2$ pressures of 1–6 MPa in 1-MPa increments. Equilibrated specimens were heated in a glycerin bath until thermal equilibrium was reached, and a steady foam structure was attained. Glycerin bath temperatures of 30–150 °C in 10 °C increments were examined. Using knowledge of gas solubility, the equation of state for $CO_2$, the effective glass-transition temperature as a function of gas concentration, and a model for mass balance within a solid-state foam, we demonstrate that foam growth terminates when sufficient gas is driven from the polycarbonate matrix into the foam cells. The foam cell walls freeze at the elevated bath temperature because of gas transport from the polycarbonate matrix and the associated rise in the polymer glass-transition temperature to that of the heated bath. © 2001 John Wiley & Sons, Inc. J Polym Sci B: Polym Phys 39: 868–880, 2001

**Keywords:** foam growth; glass-transition-temperature depression; plasticization; solid-state microcellular foams; mass transport; dual-mode gas sorption

## INTRODUCTION AND GOALS

Ever since the process to produce cells in the 2–25-$\mu$m range in polystyrene was discovered by Suh et al.[1–3] in 1984, interest in microcellular technology has been steadily growing. The original motivation for the work at the Massachusetts Institute of Technology was to reduce the material consumption in thin-walled plastic packaging products through a reduction in the density of the material. It was hypothesized that if the foam cells introduced were sufficiently small, the mechanical properties could perhaps be maintained at a level such that the product function was not compromised. Because conventional polymer foaming processes produce foam cells that are 0.25 mm or larger, a new process was sought that could produce foam cells an order of magnitude smaller if the goal of making foam parts with a wall thickness of 0.25–0.5 mm was to be achieved. Conventional processes to produce foams involve melting the polymer and then introducing a gas to form the cells. The gas may be introduced as a result of a chemical reaction (e.g., chemical blowing agent) or directly as a physical blowing agent. The resulting foam cells are relatively large in

*Correspondence to:* M. R. Holl, Department of Electrical Engineering, University of Washington, Box 352500, Seattle, WA 98195-2500 (E-mail: holl@u.washington.edu)

Journal of Polymer Science: Part B: Polymer Physics, Vol. 39, 868–880 (2001)

size, mainly because of the lower viscosity of the polymer melt at processing temperatures. To produce microcellular foams, a solid-state process was developed in which the maximum polymer temperature remains in the vicinity of the glass-transition temperature ($T_g$), well below the melting point. The plasticized but solid behavior of the polymer near the $T_g$ assists in attaining a microcellular structure.

The solid-state process consists of two distinct steps. In the first step, the polymer is exposed to a nonreacting gas at a high pressure in a pressure vessel. The gas diffuses in the polymer, eventually producing a gas-saturated specimen. Depending on the gas–polymer system and specimen thickness, the time needed to obtain a uniform gas concentration ($C$) may vary from several hours to several days. In the second step, the gas-saturated specimen is removed from the pressure vessel and heated to the foaming temperature ($T_{\text{foam}}$). This step is normally carried out in a temperature-controlled liquid bath. Heating induces the cell nucleation and growth, producing a microcellular structure. This basic process has been successful with a number of amorphous polymers, such as polystyrene, polycarbonate (PC), and poly(vinyl chloride), and semicrystalline polymers with low levels of crystallinity, such as poly(ethylene terephthalate). In each polymer, a family of foams with densities ranging from 10 to 100% of the solid polymer has been produced. A brief overview of microcellular polymers and their mechanical properties was presented by Kumar and Weller.[4] In this article, the PC–$CO_2$ system is studied in detail as an example of an amorphous solid-state gas–polymer system.

Foam cell growth in polymer melts has been studied by several researchers.[5–8] These efforts have extended earlier foam cell growth models in Newtonian fluids to the non-Newtonian polymer melts by employing suitable approximations for the melt viscosity. However, the polymer constitutive behavior in the solid-state process is fundamentally different from the melt; therefore, the available growth models are not representative of foam cell growth in this process.

In this article, we describe some new insights into the foam cell growth process in solid-state microcellular systems. A model for the characterization of steady-state foam properties (mass transport and structural) in the solid-state process was undertaken based on first principles and appropriate constitutive laws. This model, developed en route to a dynamic foam growth model, was designed with the objective of determining the overall distribution of polymer and gas within a foam structure during all quasistatic stages of the microcellular process. The insights gained from the results of this experimental and modeling effort are presented. Specifically, we show that there is a simple, self-regulating mechanism, dictated by the changing effective glass-transition temperature ($T_{g,\text{eff}}$) of the gas–polymer system, that alone determines the initiation and cessation of foam cell growth.

## BACKGROUND

The production of microcellular PC was first reported by Kumar and Weller[9,10] with $CO_2$ as the physical blowing agent. In this study, the effect of process parameters such as the $T_{\text{foam}}$, foaming time ($t_{\text{foam}}$), and saturation pressure ($P_{\text{sat}}$) of the blowing agent on the resulting microstructure was examined experimentally. An illustration of the flexibility of combining diffusion dynamics with the foam growth process was also performed to create integral polymer skin on a foamed polymer core.[11] Kumar and Weller observed that not only was the saturating gas acting as the means for cell expansion but that the plasticizing effect of the gas was also essential to the microcellular process.

Initial observations of the plasticizing effect of $CO_2$ in PC were made by Hojo and Findley in 1973.[12] Their investigation was designed to determine the effect of gas presence on the creep–creep recovery characteristics of PC that had been exposed to various nonreactive gases. They postulated that a plasticizing action had occurred because of the gas presence in the polymer. This behavior is characteristic of the free-volume theory of plasticization.[13]

The gas transport characteristics of the PC–$CO_2$ system have received considerable research attention. The characteristics examined in the literature are: (1) gas solubility, (2) gas diffusivity, (3) polymer dilation due to $C$ exposure, and (4) plasticization via the $T_{g,\text{eff}}$. Gas solubility has been described with the dual-mode sorption model.[14] In some studies, the effect of prior processing history (prior gas saturation or thermal annealing) has been examined with regard to transport.[15,16] In these studies, the dual-mode sorption model was used, and the changes in material properties due to prior gas saturation were quantified with dynamic thermal analysis traces

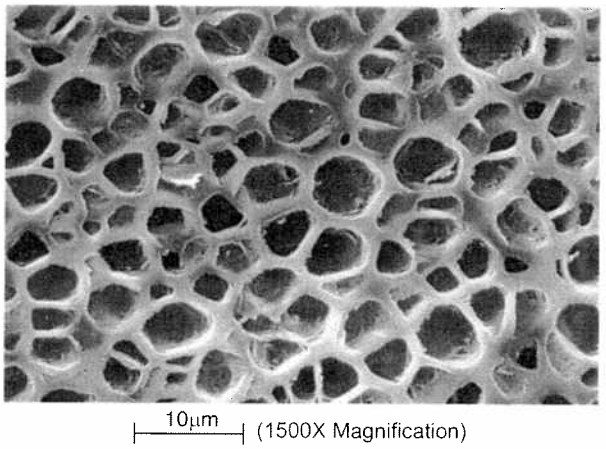


**Figure 2.** Planar intersection surface of a solid-state microcellular foam taken with a scanning electron microscope (original magnification 1500×).

the saturating gas, and (4) the $T_{g,\text{eff}}$ of the gas–polymer system.

## Gas Solubility

The dual-mode gas sorption model is used to describe the equilibrium $C$ level in polymers exposed to gases at high pressure at a specific $T_{\text{sat}}$. These isotherms are determined through experiment, and dual-mode parameters are derived from a best fit to the data. The dual-mode model is then used in the subsequent steady-state analysis. Six dual-mode gas sorption isotherms for the PC–$CO_2$ system are shown in Figure 3. The dual-mode gas sorption model for the solubility of a gas in a polymer is given as[14,15,22]

$$C(T_{\text{CV}},P_{\text{gas}}) = k_D(T_{\text{CV}})P_{\text{gas}} + \frac{C'_H(T_{\text{CV}})b(T_{\text{CV}})P_{\text{gas}}}{[1 + b(T_{\text{CV}})P_{\text{gas}}]} \quad (1)$$

where $C(T_{\text{CV}},P_{\text{gas}})$ [kg ($CO_2$)/kg (PC)] is the equilibrium gas concentration, $k_D$ {kg ($CO_2$)/[kg (PC) Pa]} is Henry's gas law constant, $C'_H$ [kg ($CO_2$)/kg (PC)] is the Langmuir capacity constant, $b$ is the Langmuir hole affinity constant (which is dimensionless), and $T_{\text{CV}}$ (K) is the temperature of the gas and polymer within the control volume.

Henry's gas constant was estimated from the experimental data and fit to a third-order polynomial of the form:

$$k_D(T_{\text{CV}}) = a_0 + a_1T_{\text{CV}} + a_2T_{\text{CV}}^2 + a_3T_{\text{CV}}^3 \quad (2)$$

The defining coefficients for eq 2 and the range of temperatures for which the coefficients are considered valid are given in Table I.

$C'_H$ was estimated from the data and then fit to a third-order polynomial of the following form:

$$C'_H(T_{\text{CV}}) = a_0 + a_1T_{\text{CV}} + a_2T_{\text{CV}}^2 + a_3T_{\text{CV}}^3 \quad (3)$$

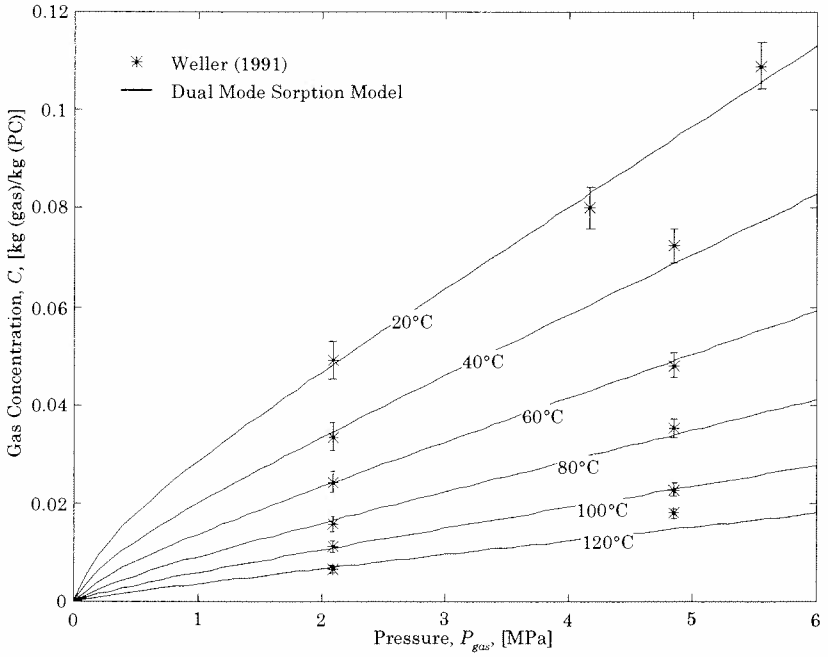


**Figure 3.** Dual-mode sorption isotherms for the PC–$CO_2$ system.

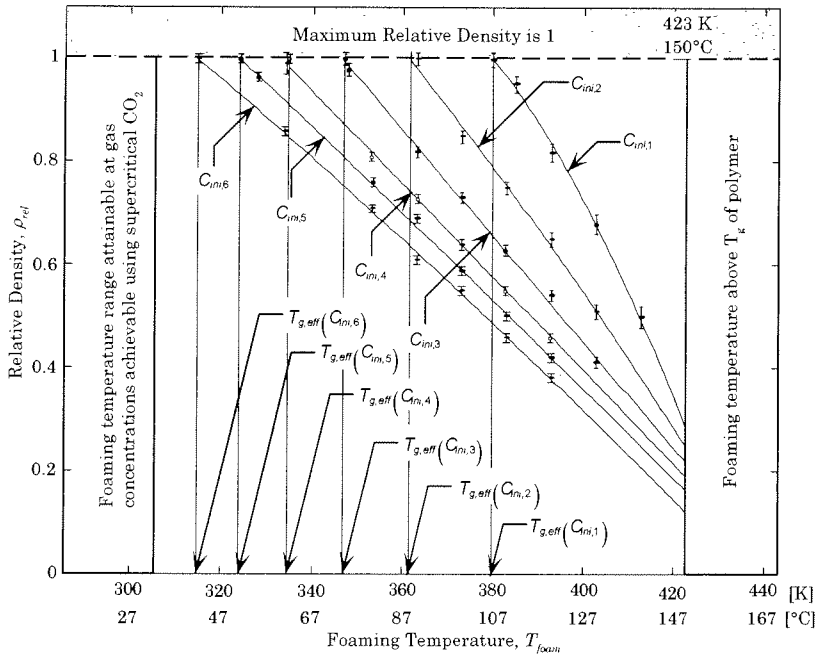


**Figure 4.** $\rho_{rel}$ as a function of $C_{ini}$ level and $T_{foam}$. See Table V for $C_{ini}$ values at different $P_{sat}$'s. All specimens were saturated as 25 °C. The intersection of the $\rho_{rel}$–$T_{foam}$ curve for a given $C_{ini}$ with $\rho_{rel} = 1.0$ gives the $T_{g,eff}$ at the corresponding $C_{ini}$. Thus, $T_{g,eff}$ for $C_{ini} = 1$ MPa is 107 °C.

where $T_{CV}$ (K) is the temperature of the gas within the cells of the control volume, $R = 8.3145$ [(N · M)/(mol · K)] is the universal gas constant, and $\bar{n}_{gas}$ (mol/m$^3$) is the molal specific volume of the gas within the cells.

The molar specific volume of a gas is the inverse of the molar $\rho_{gas}$ and is given as

$$\bar{v}_{gas}(\rho_{gas}) = \frac{MW_{gas}}{1000\rho_{gas}} \text{ (m}^3\text{/mol)} \quad (9)$$

where $MW_{gas}$ (g/mol) is the gas molecular weight. For $CO_2$, $MW_{CO_2} = 44$ g/mol.

### $T_{g,eff}$ for PC–$CO_2$

The $T_{g,eff}$ is a characteristic temperature of an amorphous polymeric material where a significant drop in strength is observed to occur. At this characteristic temperature, a segmental chain sliding motion is possible rather than just the bending of polymer backbone bond angles.[24] The Chow18 equation is used to represent the $C$ dependence of the $T_{g,eff}$ of the gas–polymer mixture:

$$T_{g,eff}(C) = T_{g0}\exp(\beta\{[1 - \theta(C)]\ln[1 - \theta(C)] + \theta(C)\ln[\theta(C)]\}) \quad (10)$$

**Table III.** Second-Order Polynomial Coefficients for Relative Density Curve Fits[a]

| $j$ | $P_{sat}$ (MPa) | $C_{ini}$ [kg ($CO_2$)/kg (PC)] | $a_{0,j}$ | $a_{1,j}$ | $a_{2,j}$ |
|---|---|---|---|---|---|
| 1 | 6.0 | 0.0260 | −14.955 | $9.4763 \times 10^{-2}$ | $-1.3889 \times 10^{-4}$ |
| 2 | 5.0 | 0.0429 | 1.8528 | $6.0151 \times 10^{-3}$ | $-2.3193 \times 10^{-5}$ |
| 3 | 4.0 | 0.0586 | 3.9999 | $-7.3736 \times 10^{-3}$ | $-3.7318 \times 10^{-6}$ |
| 4 | 3.0 | 0.0741 | 4.3460 | $-1.0828 \times 10^{-2}$ | $2.3853 \times 10^{-6}$ |
| 5 | 2.0 | 0.0895 | 3.0370 | $-4.7105 \times 10^{-3}$ | $-4.9424 \times 10^{-6}$ |
| 6 | 1.0 | 0.1047 | 2.7262 | $-3.5215 \times 10^{-3}$ | $-6.2386 \times 10^{-6}$ |

[a] The saturation temperature was 25 °C for all saturation pressures.

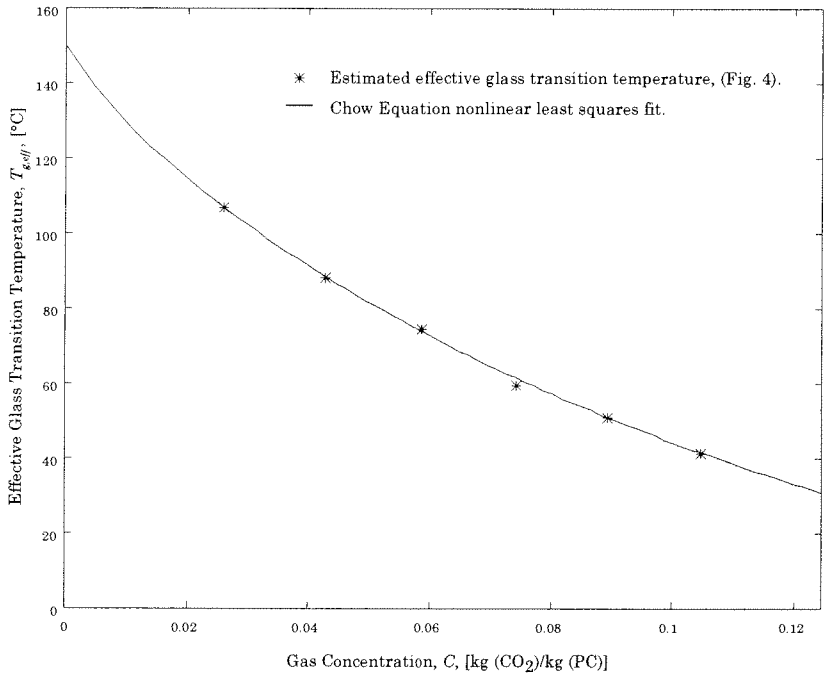


**Figure 6.** $T_{g,\text{eff}}$ as a function of the gas mass fraction; see also Kumar and Weller.[9]

Because gas mass does not cross the CV by definition, eqs 13 and 14 must be equal in magnitude. In eq 14, there is a single unknown parameter, $\rho_{\text{gas}}$. Thus, there is only one value of $\rho_{\text{gas}}$ for which eqs 13 and 14 are equivalent.

We define the normalized gas mass error function as the difference between eqs 14 and 13 divided by the volume of polymer in the sample region:

$$M_{\text{gas,CV}} = \left\{\rho_{\text{polymer,CV}}\{C[T_{\text{CV}}, P_{\text{gas}}(\rho_{\text{gas,CV}}, T_{\text{CV}})] - C_{\text{ini}}\} + \rho_{\text{gas,CV}} \frac{vf(C_{\text{ini}}, T_{\text{foam}})}{[1 - vf(C_{\text{ini}}, T_{\text{foam}})]}\right\} \quad (15)$$

Equation 15 will equal zero when the best estimate of $\rho_{\text{gas}}$ within the cells of the control volume is selected.

### Solving for Steady-State Behavior

With reference to eq 15, the following list of parameters are known for a given set of process conditions: $\rho_{\text{polymer,CV}}$, $C_{\text{ini}}$, $T_{\text{foam}}$, and $T_{\text{CV}}$. With these known parameters defined, a root search on $\tilde{\rho}_{gas,\ CV}$ in eq 15 is performed to determine the single gas density, $\rho_{\text{gas,CV}}$, for which the normalized mass error function goes to zero. With the equilibrium $\rho_{\text{gas}}$ determined, eq 8 is used to estimated the steady-state cell $P_{\text{gas}}$, and eq 1 is used to estimate the steady-state cell wall $C$ level. The $T_{g,\text{eff}}$ of the cell wall gas–polymer mixture material is determined with eq 10.

## RESULTS AND DISCUSSION

The objective is to determine the mass transport state of the foam at the moment it stops growing when $T_{\text{CV}}$ is equal to $T_{\text{foam}}$. The analysis reveals the steady-state $P_{\text{gas}}$ within the cells of the foam and $C$ within the cell walls. In this analysis, six $C_{\text{ini}}$ levels that span the range of the PC–$CO_2$ solid-state process are examined. The conditions used for the study are presented in Table V.

The steady-state mass transport analysis method was applied to the data set given in Table V over the $T_{\text{foam}}$ range that spans the process space of solid-state microcellular PC processing. $T_{\text{foam}}$ is bounded from above by the $T_g$ of unsaturated PC; the lower bound is the $T_g$ of the gas-saturated polymer. At each $C_{\text{ini}}$ level, the steady-state analysis was performed for $T_{\text{foam}}$'s greater than or equal to the $T_{g,\text{eff}}$ of the unfoamed mixture. For the analysis presented here, the control volume temperature, $\tilde{T}_{CV}$, is equal to the steady

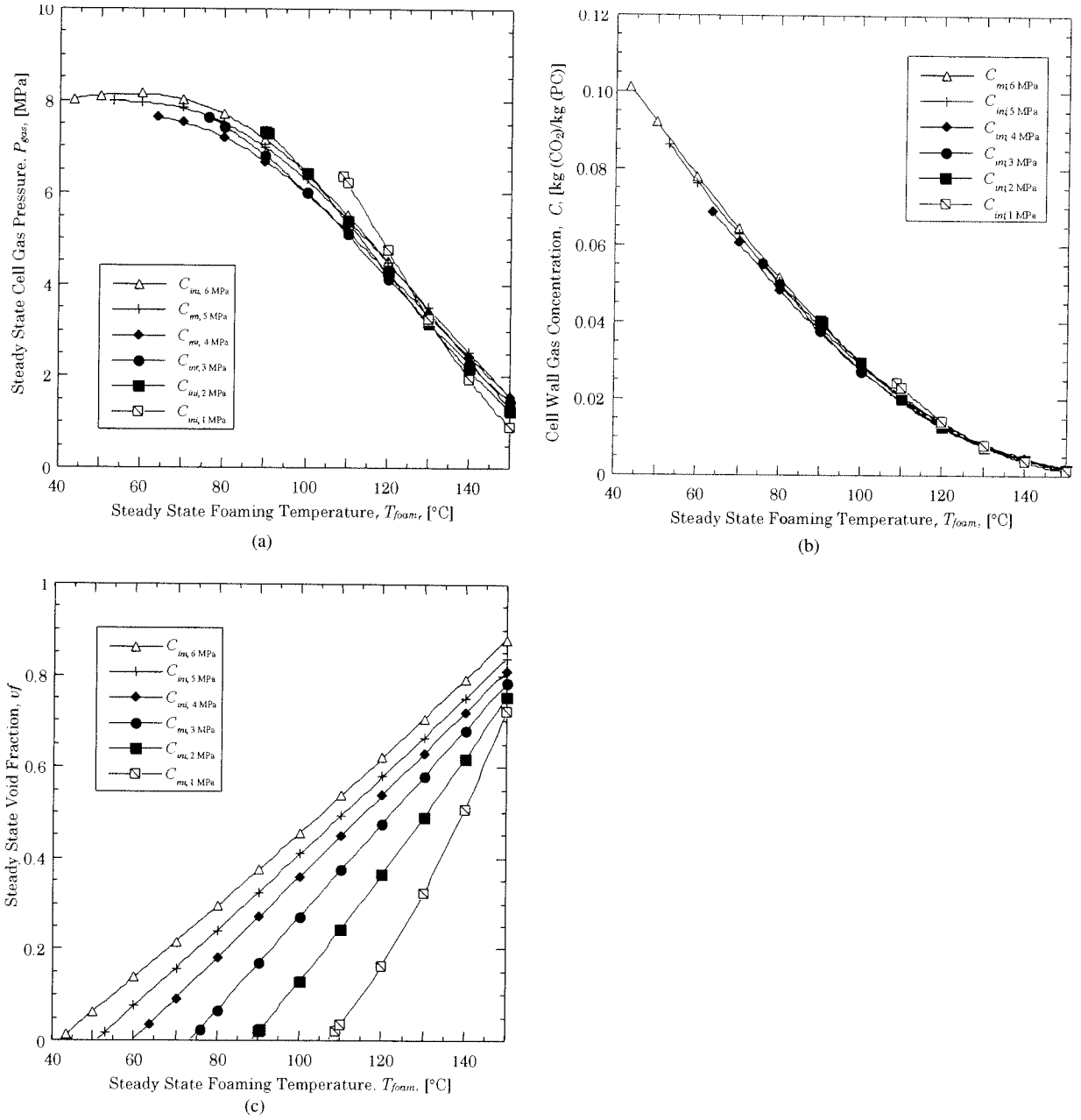


**Figure 7.** Quasi-equilibrium mass transport state for microcellular PC foam at $T_{\text{foam}}$ immediately after foam growth has stopped: (a) steady $P_{\text{gas}}$ within the cells, (b) steady $C$ in the cell walls, and (c) steady $vf$.

ature is increased through some arbitrary monotonically increasing profile to the steady $T_{\text{foam}}$, where the temperature remains constant. Cell nucleation occurs when the temperature is slightly higher than $T_{g,\text{eff}}(C_{\text{ini},4})$, and shortly thereafter, $C$ in the gas–polymer matrix begins to drop, and the strength–temperature curves begin to migrate to the right. At all times during foam expansion, the current temperature of the mixture is slightly higher than the current $T_{g,\text{eff}}$; the strength–temperature curves always lag behind the current gas–polymer mixture temperature. When the steady $T_{\text{foam}}$ is achieved by the mixture, cells will continue to grow and the strength–temperature curves will continue to shift to the right until sufficient gas has left the matrix such that the gas–polymer matrix experiences a sharp increase in the gas–polymer mixture strength. The

residual gas in the foam as a function of time and for understanding the time dependence of microcellular foam properties.

We found that regardless of $C_{ini}$, the cell wall $C$ and the cell $P_{gas}$ are the same at a given $T_{foam}$, even though different foam structures are obtained. Furthermore, a steady-state foam structure is reached when the cell wall $T_{g,eff}$ is the same as $T_{foam}$, regardless of $C_{ini}$.

These findings demonstrate the existence of a self-regulating mechanism for foam growth behavior in thermoplastic gas–polymer systems. The mechanism may be described in two parts. The first part describes the condition required for cell growth initiation, and the second part describes the condition for cell growth cessation as follows:

- Cell growth begins when the gas–polymer mixture temperature slightly exceeds the $T_{g,eff}$ of the mixture.
- Cell growth ceases when sufficient gas leaves the gas–polymer mixture during foaming such that the mixture $T_g$ is slightly less than the steady $T_{foam}$.

For $T_{foam}$'s above the $T_g$ of the virgin polymer, the self-regulating behavior disappears, and uncontrolled foam growth ensues. Thus, the microcellular structure freezes, or locks in, at the foaming bath temperature. This understanding will serve to optimize the processing conditions in a given application.

## APPENDIX: THERMOPHYSICAL PROPERTIES OF $CO_2$

The thermophysical properties of $CO_2$ and the equation of state were taken from an extensive compilation of the properties of $CO_2$.[23] When tabulated data were presented, bilinear interpolation was used.

The compressibility coefficient defines an equation of state for a gas as a function of $P_{gas}$, $T_{gas}$, and $\rho_{gas}$:

$$z(T_{gas}, \rho_{gas}) = \frac{P_{gas}\bar{v}_{gas}(\rho_{gas})}{RT_{gas}}$$

For conditions under which a gas obeys the ideal gas law, the compressibility coefficient equals unity: $z(T_{gas},\rho_{gas}) = 1$.

### Compressibility Coefficient for $CO_2$

Altunin and Gvozdkov[23] presented a very accurate (<0.3% deviation from the experiment) virial coefficient expansion representation of the equation of state (or, equivalently, the compressibility coefficient) for $CO_2$. The Altunin and Gvozdkov virial coefficient expansion coefficient representation of the compressibility coefficient for $CO_2$, with appropriate conversions for $\rho_{gas}$ in SI units, is given as follows:

$$z(T_{CO_2}, \rho_{CO_2}) = 1 + B(T_{CO_2})(1000\rho_{CO_2}) + C(T_{CO_2})(1000\rho_{CO_2})^2 + D(T_{CO_2})(1000\rho_{CO_2})^3 + E(T_{CO_2})(1000\rho_{CO_2})^4 + F(T_{CO_2})(1000\rho_{CO_2})^6 + G(T_{CO_2})(1000\rho_{CO_2})^8$$

$$B(\tau(T_{CO_2})) = 0.486590\left(1 + \frac{97}{96+\tau}\right) - (1.90843 + 5.3510\exp(-1.1576\tau))\frac{1}{\tau} - \frac{0.079526}{\tau^8}$$

$$C(\tau(T_{CO_2})) = 2.39169 - (6.96190 - 12.1824\exp(-1.1576\tau))\frac{1}{\tau} + \frac{6.86903}{\tau^2} - \frac{3.34265}{\tau^3}$$

$$D(\tau(T_{CO_2})) = -1.69007 + (10.2469 - 6.38963\exp(-1.1576\tau))\frac{1}{\tau} - \frac{14.7337}{\tau^2} + \frac{7.32711}{\tau^3}$$

$$E(\tau(T_{CO_2})) = \begin{cases} 8.69339 - \dfrac{16.9642}{\tau} + \dfrac{8.92312}{\tau^3}, & \tau \le 1.385 \\ -2.40386 + \dfrac{6.61817}{\tau} + \dfrac{9.92898}{\tau^2} - \dfrac{36.4789}{\tau^3} + \dfrac{22.0167}{\tau^4}, & \tau > 1.385 \end{cases}$$